Scientia Iranica F (2021) 28(6), 3816–3826

Sharif University of Technology
Scientia Iranica
Transactions F: Nanotechnology
http://scientiairanica.sharif.edu

Photocatalytic C-H bond activation by surface anchoring of [Co^{II}(Saloph)(His)] complex on Ag-TiO_2 nanocomposite

E. Shahnejat[a,b], and S. Mohebbi[a,b,*]

a. *Department of Chemistry, University of Kurdistan, Sanandaj, P.O. Box, 66179-416, Iran.*
b. *Research Center of Nanotechnology, University of Kurdistan, Sanandaj, P.O. Box, 66177-15175, Iran.*

Received 26 February 2021; received in revised form 27 April 2021; accepted 17 May 2021

KEYWORDS
Heterojunction catalyst;
Photocatalyst;
Alcohol oxidation;
Nanohybrid;
Plasmonic;
Cobalt Schiff base complex.

Abstract. A novel heterojunction plasmonic photocatalyst [Co(Saloph)(His)]/Ag-TiO_2 as a nanohybrid material was applied to the photocatalytic activities ranging from the C-H bond cleavage of alcohols to aldehyde using different oxidants, O_2, H_2O_2, or TBHP under irradiation of visible-light and NHPI as co-catalysts. The mentioned material was synthesized by photo-deposition of metallic silver nanoparticles on titanium oxide surface, followed by a modification of cobalt(II) Saloph complex under ultrasonic agitation conditions using a histidine linker to reach a photocatalyst under 50 nm and bandgap of 2.64 eV. The [Co(Saloph)(His)]/Ag-TiO_2 nanohybrid was characterized by EDS, XRD, DRS, FT-IR, PL spectroscopies, FESEM imaging, and BET technique. This three-component plasmonic photocatalyst revealed a high rate of photocatalytic efficiency with 95% conversion and 99% selectivity in aerobic conditions. The higher photocatalytic performance of [Co(Saloph)(His)]/Ag-TiO_2 than those of Co(Saloph)/TiO_2 and Ag-TiO_2 NPs can be attributed to Localized Surface Plasmonic Resonance (LSPR) of these motives. Therefore, this three-component nanohybrid provides an efficient interfacial electron transfer process through a synergistic effect, which in turn produces a nanocatalyst, benefiting from stability and fast selective C-H bond activation of alcohols at ambient temperature using O_2 as an inexpensive environmentally-friendly oxidant.

1. Introduction

Controlled C-H bond activation of alcohol is of great importance for chemists in the synthesis of fine chemicals, intermediates, and pharmaceutical industry [1–3]. Although several methods have been developed for C-H bond cleavage, in most of these methods, unwanted by-products have been reported. Furthermore, running the reaction in mild conditions using environmentally-friendly reagents such as molecular oxygen as oxidants and the choice of not consuming harmful or toxic organic solvents have received substantial attention [4,5].

So far, many scientists have focused on narrow bandgap semiconductors with the objective of finding a photo-assisted catalyst that can oxidize organic compounds using an alternative such as O_2. Among metal oxide semiconductors, much attention has been given to TiO_2 due to its ability to interact with atoms [6,7], tunable porous surface and distribution, high thermal stability, and cost-effective synthesis methods [8,9]. Nevertheless, its wide bandgap of 3.2

*. *Corresponding author. Tel.: +98 87 3360075*
E-mail addresses: eshahnejat@yahoo.com (E. Shahnejat), smohebbi@uok.ac.ir (S. Mohebbi)

doi: 10.24200/sci.2021.57767.5405

eV in the ultraviolet region and rapid recombination of photo-generated electrons and holes decreases the overall photocatalytic efficiency under UV-Vis electromagnetic irradiation [10]. The main drawback of these systems is the low quantum yield under visible light irradiation. Therefore, the following strategies gain significance: a) fabrication of new TiO_2 composites as a sensitive and efficient photocatalyst with the ability of high sunlight absorption and b) enhanced separation of photogenerated charges [6]. To date, numerous studies have attempted to decrease the energy bandgap and reduce the charge recombination rate to improve the photocatalytic activity of TiO_2 through metal ion grafting [11–13], surface modification [14–16], and coupling with another semiconductor [17,18]. In metal-semiconductor heterojunction, the effect of noble metal nanoparticles such as Ag, Au, Pt, and Pd can be elaborated through their surface plasmonic resonance, which is interpreted as the photoinduced collective oscillations caused by the electric field of visible light [19,20]. Incorporating silver nanoparticles into metal oxides can yield a reduction in the bandgap energy of TiO_2 to the visible spectrum as well as a reduction in the charge recombination resulting from the LSPR phenomenon [21,22]. This LSPR boosts the visible-light activity of the modified titania in the case of selective aerobic alcohol activation to aldehydes [2,23] or as antibacterial [24,25]. As shown earlier, the component of Co(Saloph)/TiO_2 nanocomposite exhibits a synergistic effect for C-H bond activation under solar light [26]. In addition, GCN/Ag-TiO_2 nanocomposite was prepared using a two-step hydrothermal process applied to the photo-degradation of methyl orange under visible light with enhanced photocatalytic activity compared to binary nanocomposites Ag-TiO_2 or GCN/TiO_2 [27]. Hence, the development of a low-cost method for the activation of molecular oxygen using a catalyst is still a challenge for scientists. Among various methods, much attention has been directed to TiO_2 immobilization. However, there are a few limited reports on surface modification or doping of TiO_2 nanoparticles with Schiff base complexes. As a result, due to the specific electronic structure of cobalt Saloph complexes, their emergence with titania might lead to a visible light sensitive catalyst.

Here, the main focus is on C-H(OH) bond oxidation of benzyl alcohol to C=O using a new ternary heterostructure nanocomposite [Co(Saloph)(His)]/Ag-TiO_2 characterized by EDS, XRD, DRS, FT-IR, and PL spectroscopies, TEM and FESEM imaging, and BET technique. Finally, the photocatalytic performance of [Co(Saloph)(His)]/Ag-TiO_2 heterojunction nanocomposite was evaluated with regard to the controlled aerobic selective oxidation alcohols to the aldehyde using NHPI as a co-catalyst through an incident visible light [28].

2. Experimental

2.1. Materials and measurements

Cobalt(II) acetate tetrahydrate 99.99%, histidine, titanium tetrachloride, silver nitrate $\geq$ 99.0%, sulfuric acid, ammonia, benzyl alcohol, acetonitrile, and hydrogen peroxide 30% were purchased from Sigma-Aldrich. Saloph, N,N′-disalicylidene-o-phenylenediimin was prepared according to the literature procedure [29]. The solvent was used after distillation and obtained from commercial sources.

Powder X-Ray Diffraction (XRD) measurements were taken by Kα, Cu radiation at 40 kV and 30 mA (λ1.5406 Å) (X-Pert Pro/Panalytical /Netherlands). Further, Fourier Transform-Infrared (FT-IR) spectra of the samples were taken on a Bruker VERTEX 80 v model using KBr pellets. Moreover, UV-Vis diffuse reflectance spectra (UV-vis-DRS) were obtained through an Avaspec-2048-TEC spectrometer at r.t. The surface morphology images were taken by a scanning electron microscope linked with an EDS for the elemental confirmation (FESEM Mira3 Tescan). The size and morphology of Saloph/Ag-TiO_2 nanoparticle were obtained by a Transmission Electron Microscopy (TEM) (CM30/Philips/Netherlands). Nitrogen adsorption-desorption analysis was determined at 77 K with a Tristar II 3020 micromeritics to report the specific surface area of the catalyst. A fluorescence spectrophotometer (Varian, Cary Eclipse, Inc.) was also used for measuring Photoluminescence (PL) spectra at ambient temperature.

2.2. Preparation of cobalt (II) Schiff base complex, Co(Saloph)

The Schiff base complex Co(Saloph) was prepared according to the methods discussed in the literature [29,30]. In general, a solution of Saloph ligand (0.316 g, 1 mmol) in ethanol (20 mL) was purged with nitrogen and heated to 60°C under a nitrogen atmosphere. A solution of one mmol cobalt(II) acetate (249 mg) in four mL methanol was gradually added to the mentioned Saloph solution to obtain black suspension. This solution was stirred and refluxed under the N2 atmosphere for 60 min. Then, a solution containing two mmol L-histidine (310 mg) in three mL water was added to the mixture and refluxed for five hours. Next, the solution was evaporated and precipitated until a dark brown solid. The solid was finally separated, washed with cool diethyl ether, and dried at room temperature.

2.3. Preparation of TiO_2 nanoparticles

In general, one mL of $TiCl_4$ was added dropwise to the solution containing four mL of 10% of sulfuric acid in an ice-water bath. After stirring for 30 min, the resulting solution was heated and kept at 85°C for 60 min [31]. Then, concentrated ammonia was added to the solution

until the supernatant liquid reached pH 7. Through the addition of ammonia, the solution was changed to white suspension. Then, the obtained gel was separated and washed several times. TiO_2 powders were dried in a vacuum oven at 30°C and finally calcined at 400°C for producing white TiO_2 nanoparticles.

2.4. Fabrication of [Co(Saloph)(His)]/Ag-TiO_2 nanohybrid

A suspension solution of TiO_2 nanoparticles in 70 mL deionized water was prepared by sonication for 40 min. Then, a typical photo deposition method was employed [32,33], and an aqueous solution containing 10 mg $AgNO_3$ in three mL water was added and placed in a water circulated reactor. After stirring and sonication for 30 min, it was irritated under UV light (400 W-ultra-violet lamp) for 20 min. Finally, a solution of one mg cobalt(II) Schiff base complex in four mL ethanol was added while being ultrasonically agitated for 40 min. The product was separated, washed, dried, and kept in dark conditions.

2.5. Photocatalytic C-H bond oxidation procedure

The photocatalytic activity of the synthesized nanoparticle was studied using a transparency photoreaction cell (15 ml). The used apparatus was equipped with a water cooling system to relieve reaction heat and prevent overheating. Herein, to the solution of aromatic alcohols (0.1 mmol) in 1.5 ml acetonitrile was added a certain amount of the photocatalyst and oxidant. Then, the photoreaction reactor was incident by a 500W Halogen lamp while being vigorously stirred. The reaction progress was followed by TLC via periodic sampling. The final solution was analyzed by gas chromatography after photocatalyst separation.

2.6. Stability of photocatalyst

The stability of the catalyst was studied by recovering and reusing the photocatalyst. The catalyst was then separated by centrifuge, washed with acetonitrile 8 times to insure the removal of the residual materials, and stored in a dark place for reusing. The recovered catalyst was reused eight times.

3. Results and discussions

3.1. Synthesis and identification of nano photocatalyst [Co(Saloph)(His)]/Ag-TiO_2

The heterostructure [Co(Saloph)(His)]/Ag-TiO_2 nanohybrid was fabricated according to the schematic preparation path in Figure 1. Here, after synthesis of the monodisperse TiO_2 nanoparticles with a size of less than 50 nm, the metallic silver was photodeposited on the surface of titan through the photoreduction process. To incorporate suitable controls in the tunability of photocatalytic behavior, optimization of both UV-light irradiation time and ratio of Ag to TiO_2 is necessary. Finally, the cobalt(II) Saloph complex was immobilized on Ag-TiO_2 nanocomposites. The [Co(Saloph)(His)] complex was obtained by the direct coordination of histidine to the cobalt center of the Saloph complex. The function of the coordinated histidine is supposed to be a linker between the cobalt Schiff base complex and the surface of TiO_2 nanoparticles to obtain a simple method. The major role of the Schiff base complex is to increase the light sensitivity of nanohybrid photocatalysts in the visible region. This heterojunction [Co(Saloph)(His)]/Ag-TiO_2 nanohybrid should enjoy the characteristics of the enhanced photocatalytic performance due to the synergic interaction that provides feasible transfer of photogenerated electron/hole pairs.

The FT-IR spectra of TiO_2 nanoparticles, Co(Saloph) complex, Ag-TiO_2 nanocomposites, and [Co(Saloph)(His)]/Ag-TiO_2 nanohybrid are shown in Figure 2. The wide vibrational band of about 490–690 cm^{-1} is ascribed to the Ti-O vibration of TiO_2 nanoparticles. The adjustment of this band as well as the appearance of new weak bands in nanohybrid

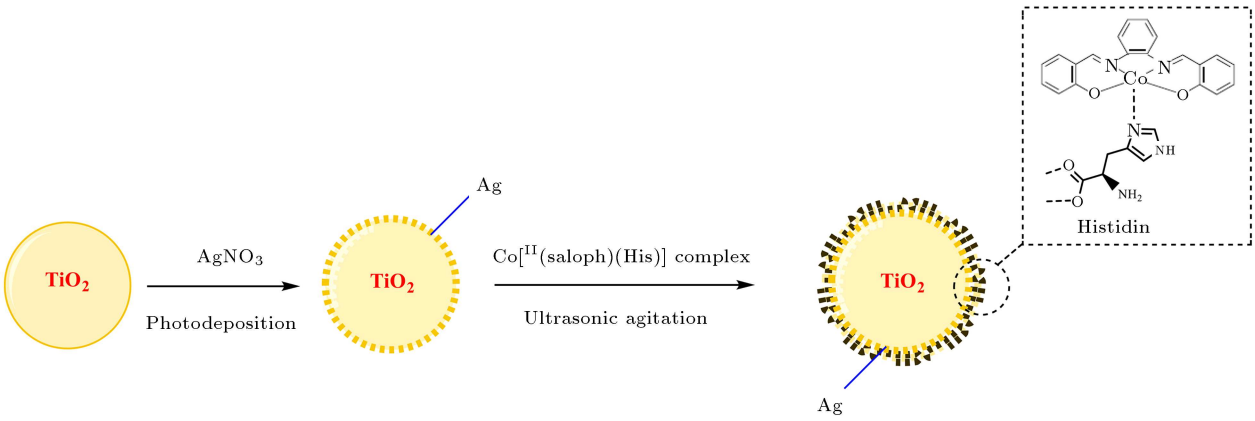

Figure 1. Schematic preparation phase of [Co(Saloph)(His)]/Ag-TiO_2 as a photocatalyst.

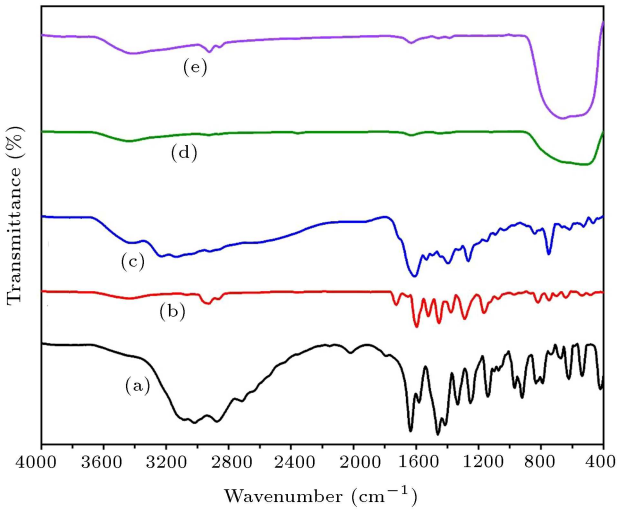

Figure 2. FT-IR spectrums: (a) Histidine, (b) Co(Saloph) complex, (c) [Co(Saloph)His] complex, (d) TiO_2 nanoparticles, and (e) [Co(Saloph)(His)]/Ag-TiO_2 nanohybrid.

result from the deposition of the cobalt Saloph complex on the surface of titania nanoparticles. A comparison between the IR spectra of the cobalt complex and those of the starting materials could be used as evidence for the formation of histidine adduct of the cobalt complex. The broadening and small changes in the vibrational wavenumber of the carboxylic group of histidine and imine bond of Schiff base complex at 1630–1730 cm^{-1} should be due to the coordination between histidine and cobalt through its carboxyl tail. Upon complexation, the vibrational band of imine shifts to lower wavenumbers [34] due to the increase of back bonding of cobalt to imine, which is the result of the coordination between histidine and cobalt. Hence, the histidine IR bands did not shift in the region of 400-1500 cm^{-1}, except the vibration band of COO- at 1416 cm^{-1}, which appeared as a broad band in this complex.

The phase composition and crystal structure of the prepared heterostructure were characterized by XRD. The powder X-ray diffraction patterns of the [Co(Saloph)(His)]/Ag-TiO_2 nanohybrid were investigated, as presented in Figure 3. The XRD pattern indicates that this sample has high crystallinity and pure crystal phase. The scattering angles at around 2θ = 25.5°, 37.2°, 48.2°, 54.1°, 55.2°, 68.9°, 62.9°, 70.4°, 75.2° are ascribed to (101), (004), (200), (105), (211), (116), (204), (220), (215) reflection planes, respectively, which identify this product as the anatase phase of TiO_2. Also, the peak at 2θ value of (38.00 or/and 38.75) is assigned to the silver. Herein, loading of the Schiff base complex as well as Ag on the surface of TiO_2 did not affect the crystalline phase of TiO_2 nanocomposite; therefore, the crystalline phase was the same as that before junction. Also, a new weak diffraction peak at the scattering angle of 2θ 32.7° in

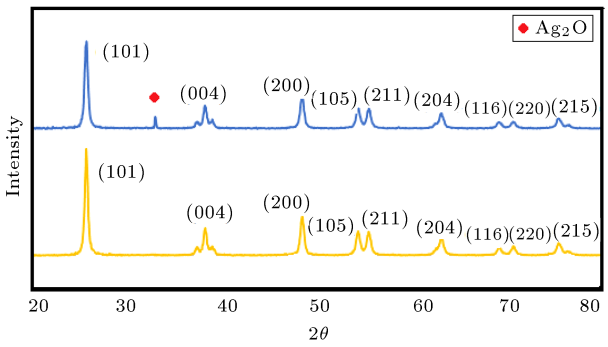

Figure 3. XRD pattern of [Co(Saloph)(His)]/Ag-TiO_2 nanohybrid: (a) Before catalytic reaction and (b) after 8 times reuse of catalyst.

[Co(Saloph)(His)]/Ag-TiO_2 nanohybrid appeared after the catalytic reaction, which could be ascribed to Ag_2O [35]. It is implied that trace Ag_2O is formed during the photodeposition process.

As shown in Figures 4 and 5, the morphology of the nanohybrid photocatalyst was determined as quasi-spherical particles by FESEM and TEM imaging, with an almost narrow size distribution of 10 to 50 nm. The FESEM images of [Co(Saloph)(His)]/Ag-TiO_2 nanohybrid show the quasi-spherical to spherical morphology. It seems that the deposition of metallic Ag and the conjunction of Schiff base complex on the surface of TiO_2 did not change the morphology of nanoparticles while a minor increase of nm sizes was observed. However, Figure 4(b) shows that the Schiff base complex has uniform dispersal on TiO_2 nanoparticles with some aggregation.

The presence of Co and Ag atoms in the nanohybrid was also confirmed by the EDX analysis, as shown in Figure 6. In Figure 6(d), in addition to TiO_2 peaks, some peaks appeared in association with Ag and cobalt elements in the nanohybrid, while these recent peaks were not seen in the spectrum of bare titania nanoparticle. Therefore, Ti, O, C, and N peaks confirmed the presence of TiO_2 particles and Schiff base and the Ag peak resulted from Ag nanoparticles. The signal at 1.5 eV is related to Al, Kα of the thin foil specimen at the sampling stage in the SEM since no other Al-based chemicals have been used throughout the synthesis. The results confirm the successful deposition of the Ag and Schiff base complex on the nanohybrid.

The value for the specific surface area of the [Co(Saloph)(His)]/Ag-TiO_2 nanohybrid was obtained from nitrogen adsorption-desorption isotherms by the BET (Brunauer-Emmett-Teller) method. The surface area of TiO_2 slightly changed after loading with Ag nanoparticles and was about 25 m^2/g.

The electronic properties of the NPs were measured using diffuse reflectance spectroscopy, UV-Vis DRS. The DRS of the [Co(Saloph)(His)]/Ag-TiO_2

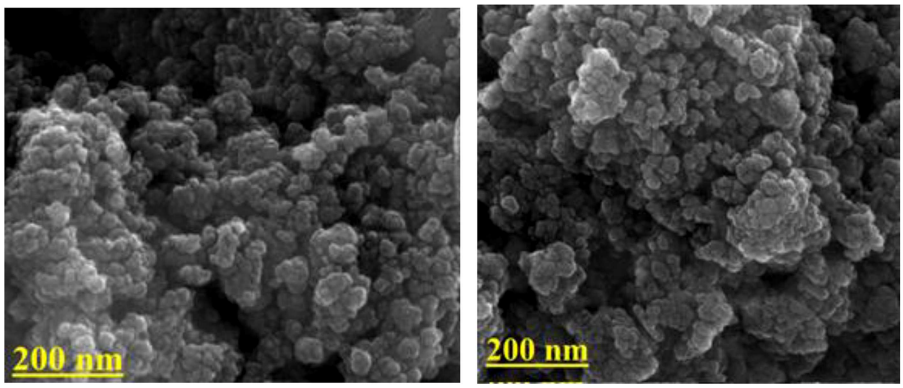

(a) (b)

Figure 4. The FE SEM imaging: (a) Ag-TiO_2 and (b) [Co(Saloph)(His)]/Ag-TiO_2 nanohybrid.

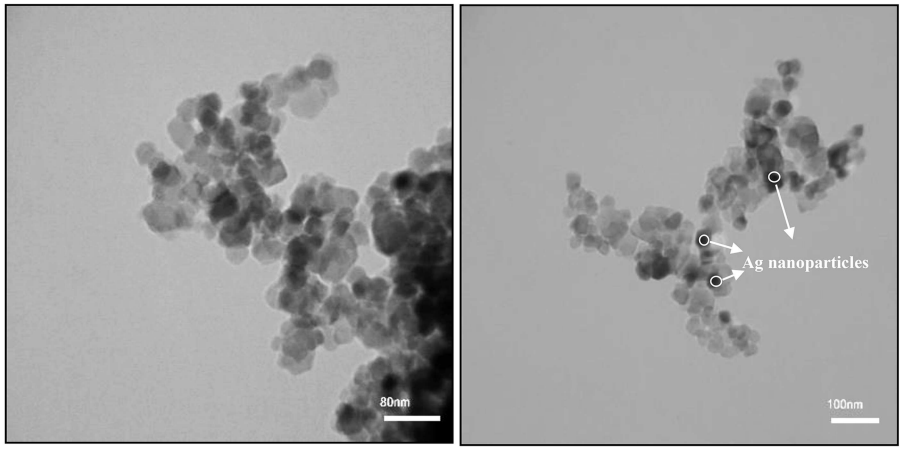

Figure 5. The TEM imaging of [Co(Saloph)(His)]/Ag-TiO_2 nanohybrid.

nanohybrid, Schiff base/TiO_2, and pure TiO_2 nanoparticle are given in Figure 7. In the TiO_2 nanoparticles, the absorption edge appears in the range of 350–390 nm (Figure 7(a)). Following the modification of the surface of pure TiO_2, the absorption intensity of visible light increased. However, in the case of [Co(Saloph)(His)]/Ag-TiO_2 nanohybrid, strong visible light edge absorption at about 640 nm and strong absorption at 460 nm could be related to the existence of both cobalt Schiff base complex and metallic Ag which almost indicate indirect and direct bandgaps at 2.14 eV and 2.65, respectively. The latter strong absorption confirmed the junction of metallic Ag to nanoparticles because the Surface Plasmonic Resonance (SPR) appeared. The [Co(Saloph)(His)]/Ag-TiO_2 photocatalyst shows greater absorption intensity in visible light, thus causing a decrease in the bandgap compared with base TiO_2. Therefore, the results reveal that the nanohybrid has excellent light absorption in the UV-Vis region (Figure 8).

3.2. Photocatalytic C-H bond activation study

The photocatalytic performance of the nanohybrid was assessed by aerobic oxidation of benzyl alcohol compared to H_2O_2, TBHP, and NHPI as the oxidant in acetonitrile under visible light irradiation. Pure TiO_2, Ag-TiO_2, Saloph/TiO_2, and [Co(Saloph)(His)]/Ag-TiO_2 nanohybrid served as control experiments for investigating photocatalytic performance. The oxidation experiment was carried out using a photocatalytic reactor irradiated under a 500 W Halogen lamp as the light source while the reaction temperature was kept at 25°C constantly. To enhance the catalytic performance of [Co(Saloph)(His)]/Ag-TiO_2 for the oxidation of alcohols, the reactions were optimized for the benzyl alcohol oxidation by influencing several aspects: catalyst amount, NHPI amount, solvent, and oxidant nature. The result is summarized in Tables 1–4.

Also, another reference photocatalytic oxidation reaction was performed using [Co(Saloph)]/TiO_2 NPs that shows significantly lower conversion percentage than [Co(Saloph)(His)]/Ag-TiO_2, even for a longer reaction time. Also, the supporting experiments confirm the crucial role of metallic silver in enhancing the reaction in such a low room temperature. The control experiment in the absence of the light was run and no detectable oxidation of alcohol was shown (Table 1). Also, the catalyst was recovered and reused eight times

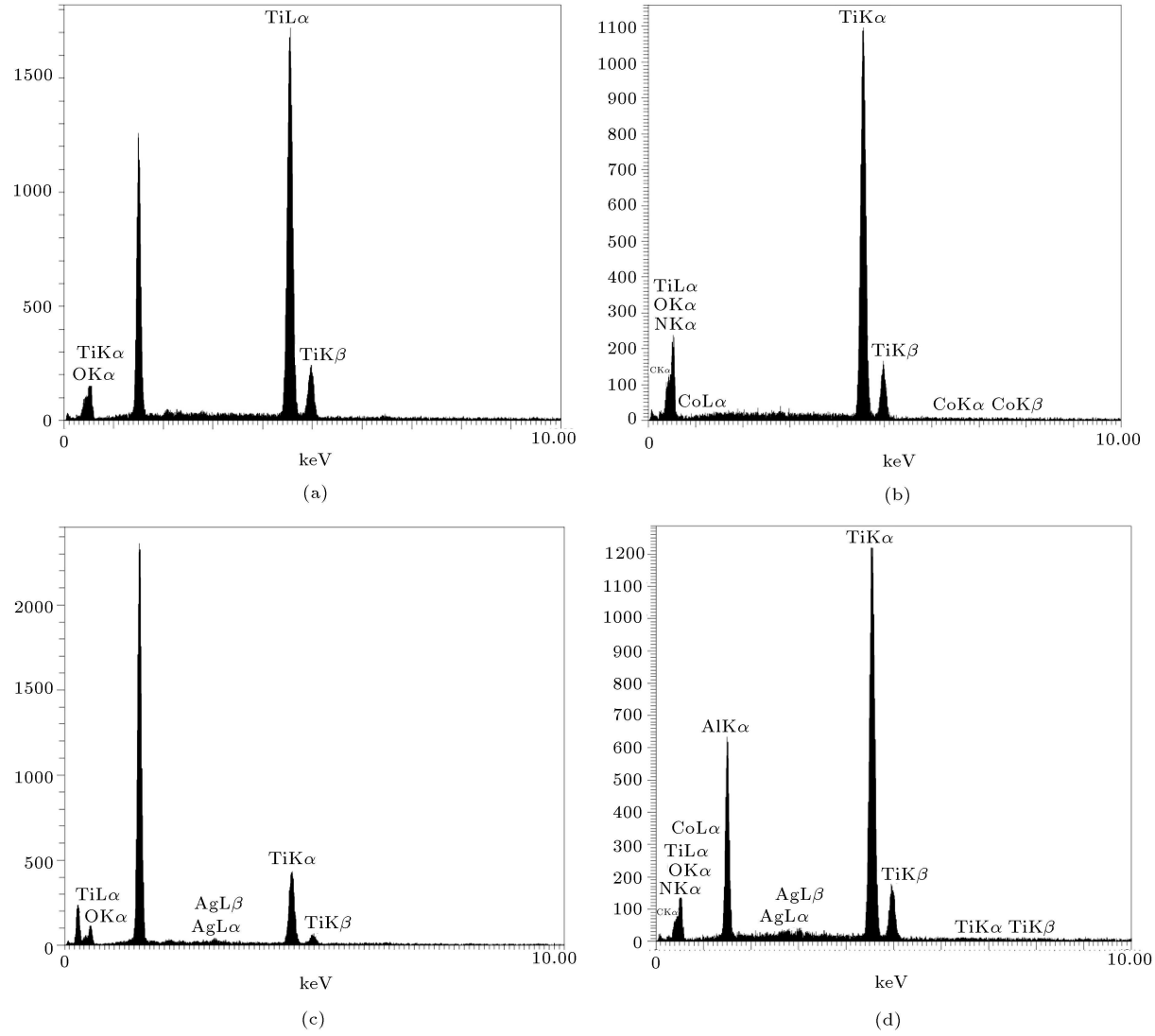

Figure 6. EDX spectrums of (a) TiO_2, (b) Ag-TiO_2, (c) Co(Saloph)/TiO_2, and (d) [Co(Saloph)(His)]/Ag-TiO_2 nanoparticles (the signal at 1.5 eV is related to Al, Kα of the SEM stage foil).

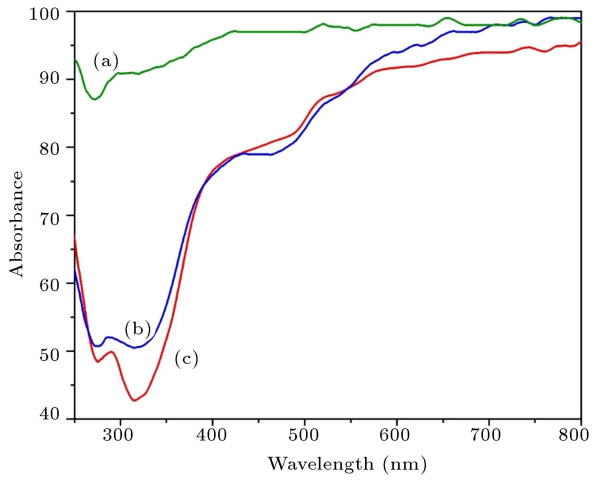

Figure 7. DRS analysis of (a) pure TiO_2 (green), (b) Co(Saloph)(His)/TiO_2 (blue) and (c) [Co(Saloph)(His)]/Ag-TiO_2 nanohybrid (red).

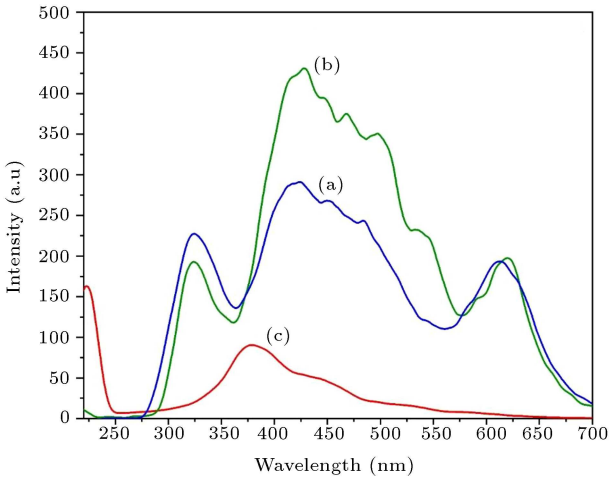

Figure 8. The photoluminescence spectra: (a) Pure TiO_2, (blue), (b) Co(Saloph)(His)/TiO_2, (green), and (c) [Co(Saloph)(His)]/Ag-TiO_2 nanoparticles, (red).

Table 1. The yield and selectivity of photo-catalytic oxidation of benzyl alcohol to benzaldehyde by incident visible light[a].

Entry	Catalyst	Amount of Catalyst (mg)	Selectivity (%)	Yield (%)
1	Pure TiO_2	5	> 99	17
2	Ag-TiO_2	5	> 99	5
3	Co(Saloph)/TiO_2	5	> 99	10
4	[Co(Saloph)(His)]/Ag-TiO_2	5	> 99	45
5	Pure TiO_2	8	> 99	30
6	Ag-TiO_2	8	> 99	40
7	Co(Saloph)/TiO_2	8	> 99	65
8	[Co(Saloph)(His)]/Ag-TiO_2	8	> 99	97
9	Pure TiO_2	10	> 99	31
10	Ag-TiO_2	10	> 99	40
11	Co(Saloph)/TiO_2	10	> 99	67
12	**[Co(Saloph)(His)]/Ag-TiO_2**	**10**	**> 99**	**91**
13	Pure TiO_2	15	> 99	37
14	Ag-TiO_2	15	> 99	42
15	Co(Saloph)/TiO_2	15	> 99	70
16	[Co(Saloph)(His)]/Ag-TiO_2	15	> 99	89
17[b]	No Catalyst	0	-	1 >

[a] Photocatalytic reaction condition: benzyl alcohol (0.1 mmol), solvent acetonitrile (1.5 ml), NHPI (8 mg), and reaction time 90 min. [b] Reaction in dark condition: The same condition as photocatalytic reaction except in the absence of light.

Table 2. The solvent effect on photocatalyst performances in aerobic benzyl alcohol oxidation[a].

Entry	Catalyst	Time (min)	Solvent	Selectivity (%)	Yield (%)
1	Pure TiO_2	90	Acetonitrile	99 >	30
2	Co(Saloph)/TiO_2	90	Acetonitrile	99 >	65
3	**[Co(Saloph)(His)]/Ag-TiO_2**	**90**	**Acetonitrile**	**99 >**	**97**
4	Pure TiO_2	90	DMF	99 >	30
5	Co(Saloph)/TiO_2	90	DMF	99 >	45
6	[Co(Saloph)(His)]/Ag-TiO_2	90	DMF	99 >	57
7	Pure TiO_2	90	CH_2Cl_2	99 >	15
8	Co(Saloph)/TiO_2	90	CH_2Cl_2	99 >	47
9	[Co(Saloph)(His)]/Ag-TiO_2	90	CH_2Cl_2	99 >	56
10	Pure TiO_2	90	H_2O	–	0
11	Co(Saloph)/TiO_2	90	H_2O	–	0
12	[Co(Saloph)(His)]/Ag-TiO_2	90	H_2O	–	0

[a]Photocatalytic reaction condition: benzyl alcohol (0.1 mmol), solvent acetonitrile (1.5 ml), NHPI (8 mg), O_2, and reaction time 90 min.

without noticeable leak of catalytic efficiency, which confirmed the stability of [Co(Saloph)(His)]/Ag-TiO_2 under photooxidation conditions.

3.3. The solvent effect on the photocatalytic oxidation of benzyl alcohol

The effect of solvents on the photocatalytic yield of benzyl alcohol oxidation was considered and the result is summarized in Table 2. The photocatalytic oxidation was performed using 8 mg of [Co(Saloph)(His)]/Ag-TiO_2 nanohybrid in optimized conditions using a variety of solvents acetonitrile, DMF, CH_2Cl_2, and water. The results indicate that acetonitrile as a solvent can provide the best environment to reach the highest conversion and selectivity for the photocatalytic oxidation of alcohol, while water shows the lowest reaction progress.

3.4. The effect of oxidant nature and amount of NHPI at photocatalytic C-H(OH) bond activation of benzyl alcohol

The effect of oxidant nature and NHPI amount for

Table 3. The effect of oxidant nature on the catalytic photo-oxidation of benzyl alcohol[a].

Entry	Catalyst	Oxidant	Product	Selectivity (%)	Yield (%)
1	Pure TiO_2	Air	Benzaldehyde	99 >	< 5
2	Co(Saloph)/TiO_2	Air	Benzaldehyde	99 >	< 5
3	[Co(Saloph)(His)]/Ag-TiO_2	Air	Benzaldehyde	99 >	< 5
4	Pure TiO_2	H_2O_2	Benzaldehyde	99 >	30
5	Co(Saloph)/TiO_2	H_2O_2	Benzaldehyde	99 >	22
6	[Co(Saloph)(His)]/Ag-TiO_2	H_2O_2	Benzaldehyde	99 >	50
7	Pure TiO_2	THBP	Benzaldehyde	99 >	34
8	Co(Saloph)/TiO_2	THBP	Benzaldehyde	99 >	50
9	[Co(Saloph)(His)]/Ag-TiO_2	THBP	Benzaldehyde	99 >	76
10	Pure TiO_2	O_2	Benzaldehyde	99 >	37
11	Co(Saloph)/TiO_2	O_2	Benzaldehyde	99 >	65
12	**[Co(Saloph)(His)]/Ag-TiO_2**	O_2	**Benzaldehyde**	**99 >**	**97**

a Photocatalytic reaction condition: benzyl alcohol (0.1 mmol), solvent acetonitrile (1.5 ml), NHPI (8 mg), [Co(Saloph)(His)]/Ag-TiO_2 (8 mg), and reaction time 90 min.

Table 4. The effect of amount of NHPI on the catalytic photo-oxidation of benzyl alcohol[a].

Entry	Catalyst	Amount of NHPI	Product	Selectivity (%)	Yield (%)
1	[Co(Saloph)(His)]/Ag-TiO_2	16 mg	Benzaldehyde	80	50
2	[Co(Saloph)(His)]/Ag-TiO_2	12 mg	Benzaldehyde	85	60
3	[Co(Saloph)(His)]/Ag-TiO_2	10 mg	Benzaldehyde	90	70
4	[Co(Saloph)(His)]/Ag-TiO_2	8 mg	Benzaldehyde	> 99	97

[a]Photocatalytic reaction condition: benzyl alcohol (0.1 mmol), solvent acetonitrile (1.5 ml), NHPI (8 mg), [Co(Saloph)(His)]/Ag-TiO_2 (8 mg), and reaction time 90 min.

catalytic photo-oxidation of benzyl alcohol was explored (Tables 3 and 4). Through the aerobic photooxidation of benzyl alcohol by [Co(Saloph)(His)]/Ag-TiO_2 in the optimized conditions of NHPI in acetonitrile, benzaldehyde-producing yield reached 97% yield within 90 min by incident visible light irradiation. The application of the higher molar ratio of NHPI (10%, 7.5%, and 6.25l%) caused over oxidation of benzyl alcohol toward benzoic acid. Therefore, under optimized conditions such as NHPI amount and by using [Co(Saloph)(His)]/Ag-TiO_2 (8 mg) and NHPI (5 mol%), 97% of benzyl alcohol was oxidized into benzaldehyde with excellent selectivity (> 99) in 90 min in acetonitrile.

3.5. Plausible photocatalytic electron transfer mechanism in [Co(Saloph)(His)]/Ag-TiO_2

Photoluminescence (PL) spectroscopy is extensively used to detect the charge migration and recombination process of photoinduced e^-h^+ exciton pairs. According to Figure 8, Co(Saloph)/TiO_2 and TiO_2 NPs exhibit similar luminescence spectra, which were compared with [Co(Saloph)(His)]/Ag-TiO_2 nanohybrid in different excitation wavelength numbers. The PL spectra of pure TiO_2 and Schiff base/TiO_2 nanoparticles have strong emission peaks, which are assigned to the fast recombination of the electron holes of these samples. Low photoluminescence intensity results from the lower recombination rate of exciton pairs $h^+ - e^-$, which should improve the performance of photocatalytic reaction. The photoluminescence intensity of [Co(Saloph)(His)]/Ag-TiO_2 nanocomposite exhibits significant quenching in comparison with pure TiO_2 and/ or Schiff base/TiO_2 nanocomposite. However, the PL quenching behavior of the [Co(Saloph)(His)]/Ag-TiO_2 nanohybrid reveals a lower charge recombination rate than base NPs. Thus, the high photoactivity of the [Co(Saloph)(His)]/Ag-TiO_2 nanohybrid is consistent with its efficient charge separation. Variation in PL intensities are an argument to prove the crucial role of the [Co(Saloph)(His)]/Ag-TiO_2 nanohybrid in blocking the recombination of charge carriers. Silver dots play as a conduction bridge to facilitate electron transfer and reduce the charge recombination rate of photogenerated exciton pair electron-hole. Also, the high catalytic performance of this photooxidation system

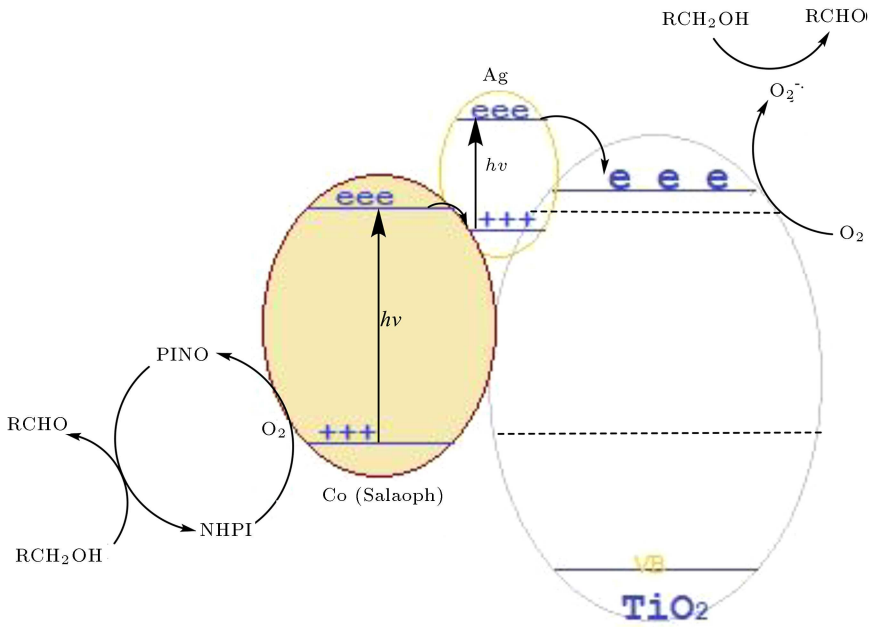

Figure 9. Schematic plausible photocatalytic electron transfer mechanism in [Co(Saloph)(His)]/Ag-TiO_2.

is dependent on such conditions in which molecular oxygen is used to accompany NHPI, while O_2 itself is not enough to play an oxidative role. From a mechanistic point of view, the NHPI plays the role of a radical initiator through forming an active radical species phthalimide-N-oxyl (PINO) [36,37]. Thus, a reliable plausible mechanism should be accomplished with this active intermediate to improve the catalytic oxidation process (Figure 9).

3.6. Stability of the photocatalyst [Co(Saloph)(His)]/Ag-TiO_2

Besides, the stability of the catalyst was studied by performing catalytic reaction several times. Therefore, the [Co(Saloph)(His)]/Ag-TiO_2 photocatalyst was used consecutively eight times for the selective catalytic photo-oxidation of benzyl alcohol. Fortunately, change in conversion percentages was negligible, which could establish the stability of this nanohybrid catalyst in photo-oxidation conditions. As shown in Figure 10, photocatalysts exhibited high stability during reusing without significant loss of catalytic activity [Co(Saloph)(His)]/Ag-TiO_2. Also, as shown in Figure 3, the comparison of the XRD pattern of the catalyst before reaction and after eight times reusing did not show detectable change; therefore, the nanohybrid exhibited excellent stability under irradiation of visible light.

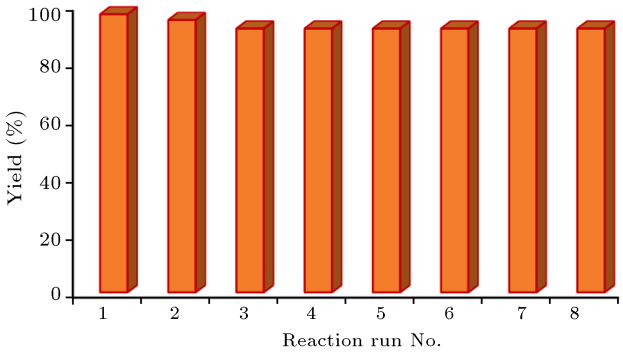

Figure 10. Reuse of the [Co(Saloph)(His)]/Ag-TiO_2 photocatalyst in the oxidation reaction of benzyl alcohol.

4. Conclusions

This study attempted to conduct successful fabrication of a nanohybrid [Co(Saloph)(His)]/Ag-TiO_2 as a photocatalyst by modifying the surface of doped anatase phase Ag-TiO_2 nanocomposite with size under 50 nm by anchoring a cobalt Schiff base complex through histidine as the linker and it was characterized by EDS, XRD, DRS, FT-IR, PL spectroscopies, FESEM imaging, and BET technique. The Ag-TiO_2 nanocomposites were obtained through the photoreduction of silver ions on the surface of TiO_2 nanoparticles. This three-component heterostructure nanohybrid shows the indirect bandgap 2.14 eV and direct bandgap 2.65 eV as well as a significant enhanced photocatalytic activity with 95% conversion and 99% selectivity in aerobic conditions toward controlled C-H bond activation of benzyl alcohol to form C=O bond in benzaldehyde under visible light irradiation. The photocatalytic performance was enhanced compared with Ag-TiO_2 or TiO_2 nanoparticles or immobilized TiO_2 with cobalt Saloph complex. It seems that metallic Ag creates a synergic connection between other components of this

system and could facilitate electron transfer through its surface plasmonic effect. Therefore, these results demonstrate the interfacial junction of Ag-TiO_2 with the cobalt Schiff base complex that causes efficient charge separation. As a result, this separation of photogenerated carriers' holes/electrons reduces the charge recombination rate to reach higher photocatalytic activities. Moreover, the [Co(Saloph)(His)]/Ag-TiO_2 nanohybrid exhibited excellent stability under irradiation of visible light.

Acknowledgments

The University of Kurdistan is acknowledged for rendering financial support of this research.

References

1. Liu, M., Wang, H., Zeng, H., and Li, C.J. "Silver(I) as a widely applicable, homogeneous catalyst for aerobic oxidation of aldehydes toward carboxylic acids in water-"silver mirror": From stoichiometric to catalytic", *Sci. Adv.*, **1**(2), p. e1500020 (2015).
2. Enache, D.I., Edwards, J.K., Landon, P., Solsona-Espriu, B., Carley, A.F., Herzing, A.A., Watanabe, M., Kiely, C.J., Knight, D.W., and Hutchings, G.J. "Solvent-free oxidation of primary alcohols to aldehydes using Au-Pd/TiO_2 catalyst", *Science*, **311**(5759), pp. 362—365 (2006).
3. Palmisano, G., Yurdakal, S., Augugliaro, V., Loddo, V., and Palmisano, L. "Photocatalytic selective oxidation of 4-methoxybenzyl alcohol to aldehyde in aqueous suspension of home-prepared titanium dioxide catalyst", *Adv. Synth. Catal.*, **349**(6), pp. 964–970 (2007).
4. Ten Brink, G.J., Arends, I.W.C.E., and Sheldon, R.A. "Green, catalytic oxidation of alcohols in water", *Science*, **287**(5458), pp. 1636–1639 (2000).
5. Lang, X., Ma, W., Chen, C., Ji, H., and Zhao, J. "Selective aerobic oxidation mediated by TiO_2 photocatalysis", *Acc. Chem. Res.*, **47**(2), pp. 355–363 (2014).
6. Li, W., Wu, Z., Wang, J., Elzatahry, A.A., and Zhao, D. "A perspective on mesoporous TiO_2 materials", *Chem. Mater.*, **26**(1), pp. 287–298 (2014).
7. Meng, A., Zhang, L., Cheng, B., and Yu, J. "Dual cocatalysts in TiO_2 photocatalysis", *Adv. Mater.*, **31**(30), p. 1807660 (2019).
8. Bagheri, S., Muhd Julkapli, N., and Bee Abd Hamid, S. "Titanium dioxide as a catalyst support in heterogeneous catalysis", *Sci. World J.*, **2014**, Article ID 727496, 21 pages (2014). http://dx.doi.org/10.1155/2014/727496
9. Zhou, R., Lin, S., Zong, H., Huang, T., Li, F., Pan, J., and Cui, J. "Continuous synthesis of Ag/TiO_2 nanoparticles with enhanced photocatalytic activity by pulsed laser ablation", *J. Nanomater*, **2017**, Article ID 4604159 (2017). https://doi.org/10.1155/2017/4604159
10. Subramanian, V., Wolf, E., and Kamat, P.V. "Semiconductor-metal composite nanostructures. To what extent do metal nanoparticles improve the photocatalytic activity of TiO_2 films?", *J. Phys. Chem. B.*, **105**(46), pp. 11439–11446 (2001).
11. Kisch, H. "Semiconductor photocatalysis-mechanistic and synthetic aspects", *Angew. Chemie-Int. Ed.*, **52**(3), pp. 812–847 (2013).
12. Irie, H., Miura, S., Kamiya, K., and Hashimoto, K. "Efficient visible light-sensitive photocatalysts: Grafting Cu(II) ions onto TiO_2 and WO_3 photocatalysts", *Chem. Phys. Lett.*, **457**(1–3), pp. 202–205 (2008).
13. Kisch, H., Zang, L., Lange, C., Maier, W.F., Antonius, C., and Meissner, D. "Modified, amorphous titania-A hybrid semiconductor for detoxification and current generation by visible light", *Angew. Chemie-Int. Ed.*, **37**(21), pp. 3034–3036 (1998).
14. Jin, Q., Arimoto, H., Fujishima, M., and Tada, H. "Manganese oxide-surface modified titanium (IV) dioxide as environmental catalyst", *Catalysts*, **3**(2), pp. 444–454 (2013).
15. Sang, L., Zhao, Y., and Burda, C. "TiO_2nanoparticles as functional building blocks", *Chem. Rev.*, **114**(19), pp. 9283–9318 (2014).
16. Al Jitan, S., Palmisano, G., and Garlisi, C. "Synthesis and surface modification of TiO_2-based photocatalysts for the conversion of CO_2", *Catalysts*, **10**(2), p. 227 (2020).
17. Chen, Y.-C.C., Pu, Y.-C.C., and Hsu, Y.-J.J. "Interfacial charge carrier dynamics of the three-component In 2O 3-TiO 2-Pt heterojunction system", *J. Phys. Chem. C.*, **116**(4), pp. 2967–2975 (2012).
18. Habibi-Yangjeh, A., Feizpoor, S., Seifzadeh, D., and Ghosh, S. "Improving visible-light-induced photocatalytic ability of TiO_2 through coupling with Bi_3O_4Cl and carbon dot nanoparticles", *Sep. Purif. Technol.*, **238**(December), p. 116404 (2020).
19. Tian, Y. and Tatsuma, T. "Mechanisms and applications of plasmon-induced charge separation at TiO_2 films loaded with gold nanoparticles", *J. Am. Chem. Soc.*, **127**(20), pp. 7632–7637 (2005).
20. Elemike, E.E., Onwudiwe, D.C., Wei, L., Chaogang, L., and Zhiwei, Z. "Noble metal-semiconductor nanocomposites for optical, energy and electronics applications", *Sol. Energy Mater. Sol. Cells*, **201**(March), p. 110106 (2019).
21. Schneider, J., Matsuoka, M., Takeuchi, M., Zhang, J., Horiuchi, Y., Anpo, M., and Bahnemann, D.W. "Understanding TiO_2 photocatalysis: Mechanisms and materials", *Chem. Rev.*, **114**(19), pp. 9919–9986 (2014).

22. Fattahi, A., Arlos, M.J., Bragg, L.M., Liang, R., Zhou, N., and Servos, M.R. "Degradation of natural organic matter using Ag-P25 photocatalyst under continuous and periodic irradiation of 405 and 365 nm UV-LEDs", *J. Environ. Chem. Eng.*, **9**(1), p. 104844 (2021).

23. Higashimoto, S. "Titanium-dioxide-based visible-light-sensitive photocatalysis: Mechanistic insight and applications", *Catalysts*, **9**(2), p. 201 (2019).

24. Muflikhun, M.A., Frommelt, M.C., Farman, M., Chua, A.Y., and Santos, G.N.C. "Structures, mechanical properties and antibacterial activity of Ag/TiO_2 nanocomposite materials synthesized via HVPG technique for coating application", *Heliyon*, **5**(4), p. e01475 (2019).

25. Muflikhun, M.A., Chua, A.Y., and Santos, G.N.C. "Structures, morphological control, and antibacterial performance of Ag/TiO 2 micro-nanocomposite materials", *Adv. Mater. Sci. Eng.*, 2019, pp. 1–12 (2019).

26. Jafarpour, M., Kargar, H., and Rezaeifard, A. "A synergistic effect of a cobalt Schiff base complex and TiO_2 nanoparticles on aerobic olefin epoxidation", *RSC Adv.*, **6**(82), pp. 79085–79089 (2016).

27. Chen, Y., Huang, W., He, D., Situ, Y., and Huang, H. "Construction of heterostructured g-C_3N_4/Ag/TiO_2 microspheres with enhanced photocatalysis performance under visible-light irradiation", *ACS Appl. Mater. Interfaces*, **6**(16), pp. 14405–14414 (2014).

28. Hoque, M.A. and Guzman, M.I. "Photocatalytic activity: Experimental features to report in heterogeneous photocatalysis", *Materials (Basel)*, **11**(10), pp. 1–11 (2018). http://dx.doi.org/10.3390/ma11101990

29. Sarvestani, A.H. and Mohebbi, S. "Spectroscopy and electrochemistry of cobalt(III) salophen complexes", *J. Chem. Res.*, (**4**), pp. 257–260 (2006).

30. Boghaei, D.M. and Mohebi, S. "Novel unsymmetrical tetradentate Schiff base complexes of cobalt(II) and palladium(II) with N_2O_2 donor sets", *J. Chem. Res.-Part S*, (**6**), pp. 224–226 (2001).

31. Safaei, E. and Mohebbi, S. "Photocatalytic activity of nanohybrid Co-TCPP@TiO_2/WO_3 in aerobic oxidation of alcohols under visible light", *J. Mater. Chem. A.*, **4**(10), pp. 3933–3946 (2016).

32. Ghobadifard, M. and Mohebbi, S., "Novel nanomagnetic Ag/β-Ag_2WO_4/$CoFe_2O_4$ as a highly efficient photocatalyst under visible light irradiation", *New J. Chem.*, **42**(12), pp. 9530–9542 (2018).

33. Askari, P., Mohebbi, S., and Do, T.O. "High performance plasmonic activation of Ag on β-Ag_2WO_4/$BiVO_4$ as nanophotocatalyst for oxidation of alcohols by incident visible light", *J. Photochem. Photobiol. A Chem.*, **367**, pp. 56–65 (2018).

34. Mohebbi, S., Bahrami, S., and Shangaie, A. "Heterotrinuclear manganese(II) and vanadium(IV) Schiff base complexes as epoxidation catalysts", *Transit. Met. Chem.*, **36**(4), pp. 425–431 (2011).

35. Cai, T., Liu, Y., Wang, L., Zhang, S., Ma, J., Dong, W., Zeng, Y., Yuan, J., Liu, C., and Luo, S. "Dark deposition' of Ag nanoparticles on TiO_2: Improvement of electron storage capacity to boost 'memory Catalysis' activity", *ACS Appl. Mater. Interfaces*, **10**(30), pp. 25350–25359 (2018).

36. Zhao, H., Sun, W., Miao, C., and Zhao, Q. "Aerobic oxidation of secondary alcohols using NHPI and iron salt as catalysts at room temperature", *J. Mol. Catal. A Chem.*, **393**, pp. 62–67 (2014).

37. Ishii, Y., Sakaguchi, S., and Iwahama, T. "Innovation of hydrocarbon oxidation with molecular oxygen and related reactions", *Adv. Synth. Catal.*, **343**(5), pp. 393–427 (2001).

Biographies

Elham Shahnejat is a PhD Candidate in the field of inorganic chemistry at the Chemistry Department, University of Kurdistan under supervision of Professor S. Mohebbi. She has focused on functionalization of nanoparticles through linkage of coordination complexes using multi dentate ligands such as Schiff bases and porphyrin derivative and using a photocatalyst for selective oxidation of hydrocarbons.

Sajjad Mohebbi as a Professor of Chemistry and a faculty member has been working at the Chemistry Department, University of Kurdistan since 2002. His field of study is inorganic chemistry, especially inorganic catalysts and nanomaterials. His research group has focused on the preparation of new inorganic materials including coordination compound, nanoparticles and quantum dots with a broad applicability as catalysts, photocatalysts, and electro catalysts toward selective oxidation of materials, degradation of dyes, removal of pollution, and finally water splitting. His new direction approach is applied to heterogenizing homogeneous catalysts and hybrid catalysts.